Journal of New Technology and Materials
JNTM
Vol. 06, N°01 (2016)34-41

OEB Univ. Publish. Co.

Electronic structure and Fano's antiresonance study of Cr^{3+} doped BIGaZYTZr fluoride glass

Hajer Souissi[1*], Olfa Taktak[1], Olfa Maalej[2] and Souha Kammoun[1]

[1]*Laboratoire de Physique Appliquée, Groupe de Physique des Matériaux Luminescents, Université de Sfax, Faculté des Sciences de Sfax, BP 1171, 3000, Sfax, Tunisia.*

[2]*Laboratoire de Chimie Inorganique, Université de Sfax, Faculté des Sciences de Sfax, BP 1171, 3000, Sfax, Tunisia.*

souissi_hajer_fss@yahoo.fr

Received date: May 06, 2016; revised date: June 28, 2016; accepted date: June 28, 2016

Abstract

The absorption spectrum of Cr^{3+} in BIGaZYTZr ($30BaF_2$-$18InF_3$-$12GaF_3$-$20ZnF_2$-$10YF_3$-$6ThF_4$-$4ZrF_4$) fluoride glass is characterized by the presence of features on the $^4T_{2g}(^4F)$ absorption band. These features result from interaction of the $^2E_g(^2G)$ and $^2T_{1g}(^2G)$ sharp levels with the vibrationally broadened $^4T_{2g}(^4F)$ quasi-continuum via spin-orbit coupling. We have analyzed this phenomenon in the frame of the Fano's antiresonance model. This analysis permits us to determine the electronic structure of the chromium ion Cr^{3+} by the crystal field theory. A good agreement between the theoretical and the experimental energy levels are obtained. The fitted parameters by Fano's antiresonance model and the crystal field parameters obtained in this work are compared with those of homologous fluoride glasses.

Keywords: Crystal field, transition-metal, fluoride glass, interference dip, Fano's antiresonances.

1. Introduction

Considerable interest has been devoted to fluoride glasses, particularly heavy metal fluoride glasses. The optical properties of fluoride glasses are important for accurately designing optical systems, optical fiber waveguides, fiber lasers and amplifiers [1-5]. Furthermore, the ease of preparation, high concentrations of transition-metal ions can be incorporated into these matrices. These doping ions present favorable spectroscopic properties. Cr^{3+} doped glasses have attracted much attention over the past few years because of applications to lasers [6] and solar concentrators [7]. The states of transition metals in host glasses are known to be influenced by several parameters such as type and glass composition.

The optical absorption spectrum of Cr^{3+} doped BIGaZYTZr ($30BaF_2$-$18InF_3$-$12GaF_3$-$20ZnF_2$-$10YF_3$-$10ThF_4$-$4ZrF_4$) fluoride glass was measured by Elejalde *et al.* [8]. This spectrum consists of broad absorption bands with the presence of features which are attributed to the d-d transitions of the active center Cr^{3+} with $3d^3$ configuration. It is approved that in most glasses, Cr^{3+} ions occupy sites having nearly perfect octahedral symmetry because of the strong ligand field stabilization energy of Cr^{3+} in six-fold coordination [9].

In this paper, we are interested in studying the absorption spectrum of Cr^{3+} doped BIGaZYTZr fluoride glass. In the first part, we give a qualitative study of the interaction between quartet $^4T_{2g}(^4F)$ and doublet $^2E_g(^2G)$ excited levels via spin-orbit coupling by using the notion of adiabatic potential energy surfaces. In the second part, we concentrated our study on the features observed at the long wavelength $^4A_{2g}(^4F) \rightarrow {}^4T_{2g}(^4F)$ absorption band of Cr^{3+} doped BIGaZYTZr. These features have been analyzed by Fano's antiresonance model [10-11]. Finally, we present a detailed crystal-field analysis of the electronic energy levels of Cr^{3+}:BIGaZYTZr based on the Racah theory. This theoretical analysis leads to the Racah and crystal-field parameters for this ion. The splitting of the Stark levels under spin-orbit interaction is also considered. By comparison with other fluoride glasses, we tried to deduce informations such as the intensity of the crystal-field on Cr^{3+} ion (from Dq parameter) as a

function of the glass composition, the disorder in these glasses, etc....

2. Experimental Support

The spectroscopic properties of Cr^{3+} in BIGaZYTZr ($30BaF_2$-$18InF_3$-$12GaF_3$-$20ZnF_2$-$10YF_3$-$6ThF_4$-$4ZrF_4$) fluoride glass has been investigated by Elejalde *et al.* [8]. The optical absorption spectra measured by these authors will be used for the theoretical study of this article.

Figure 1 presents the room temperature absorption spectrum of Cr^{3+} (0.2 mol%) doped BIGaZYTZr fluoride glass. The absorption spectrum is characterized by two spin-allowed broad bands centered at 15391 and 22423 cm^{-1}, which are attributed respectively to the vibronically broadened transitions $^4A_{2g}(^4F) \rightarrow {}^4T_{2g}(^4F)$ and $^4A_{2g}(^4F) \rightarrow {}^4T_{1g}(^4F)$. The $^4A_{2g}(^4F) \rightarrow {}^4T_{2g}(^4F)$ absorption band shows a fine structure due to the spin-forbidden $^4A_{2g}(^4F) \rightarrow {}^2E_g(^2G)$ and $^4A_{2g}(^4F) \rightarrow {}^2T_{1g}(^2G)$ transitions.

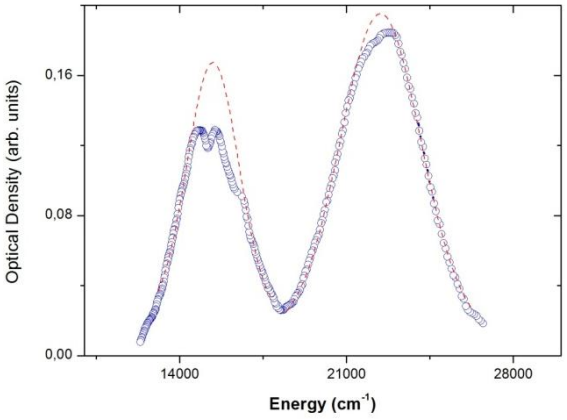

Figure 1. Optical absorption spectra of Cr^{3+} doped BIGaZYTZr fluoride glass (plotted line) at room temperature and fits to a Gaussian function (dashed line) [8].

3. Theoretical Background

The fine structure observed on the $^4A_{2g}(^4F) \rightarrow {}^4T_{2g}(^4F)$ absorption band of Cr^{3+} doped BIGaZYTZr fluoride glass will be analyzed following the Fano's antiresonance model. Then, the electronic structure is determined by the crystal field theory which reposes on the Racah tensor algebraic methods. In this section, we remember briefly the Fano's antiresonance and crystal field theories.

3.1. Fano's antiresonance method

Antiresonances features are analyzed by means of the Fano's profile function R(ω). This function is obtained from the ratio of the experimental absorption spectrum to the background spectrum, the latter being obtained by fitting the wings of the experimental absorption spectrum with a Gaussian function. In the notation of Sturge *et al.,* the Fano's theory is provided as [12]:

$$R(\omega) = 1 + \sum_i \rho_i^2 \frac{q_i^2 + 2q_i\xi_i^2 - 1}{1 + \xi_i^2} \qquad (1)$$

where:

$$\xi = \frac{\omega - \omega_{ri}}{\gamma_i}, \qquad q_i = \frac{\langle \phi_i | z | \psi_0 \rangle}{\sqrt{\pi\gamma_i}\rho_i \left\langle \psi_{E_i}^{(d)} \middle| z \middle| \psi_0 \right\rangle}$$

$$\gamma_i = \pi \left| \left\langle \psi_{E_i}^{(a)} \middle| H_i \middle| \varphi_i \right\rangle \right|, \qquad \rho_i = \left\langle \psi_{E_i}^{(a)} \middle| \psi_{E_i}^{(d)} \right\rangle$$

The index i ranges over the number of sharp levels (two in our case, i =1 for ^2E_g (^2G) and i =2 for $^2T_{1g}$ (^2G)). Interactions between these sharp levels and the vibrationally broadened $^4T_{2g}$ (^4F) are neglected. φ_i is the wave function of the sharp level in the absence of the interaction H_i with the continuum (spin-orbit in our case). Φ_i represents a modification of φ_i by the continuum and ψ_0 the ground state. z is the optical operator (electric or magnetic dipole). $\psi_{E_i}^{(a)}$ and $\psi_{E_i}^{(d)}$ arise, respectively, by auto-ionisation of φ_i and by direct transition from ground state ψ_0.

The four parameters ρ_i^2, γ_i, q_i and ω_{ri} are to be fitted. The parameter ρ_i^2 gives the fraction of the band states that take part in the interference process. γ_i indicates the spectral width of the sharp state (^2E_g or $^2T_{1g}$). q_i is a numerical index which characterizes the line profile. A value of q_i close to zero corresponds to a "true" antiresonance. Finally ω_{ri} is the resonance energy which is slightly shifted due to the interaction with the continuum, compared to the resonance energy for the unperturbed sharp absorption line.

3.2. Crystal field study of the Cr^{3+} in phosphate glasses

The total Hamiltonian of a $3d^N$ ion in an arbitrary symmetry site is written as [13,14]:

$$H = H_0 + H_{Trees} + H_{CF} + H_{SO} \qquad (2)$$

H_0 is the Coulomb interaction including electron-electron repulsions. This Hamiltonian gives the ^{2S+1}L terms: two quartet terms (^4F ground state and ^4P excited state) and six doublet excited terms (^2H, ^2G, ^2F, ^2_aD, ^2_bD and ^2P) for Cr^{3+} with a $3d^3$ configuration. The eigenvalues of Hamiltonian H_0 are expressed as a function of the Racah parameters B and C [13,15]. H_{Trees} is the Trees correction describing the two-body orbit-orbit polarization interaction (α is the Trees parameter) [16,17]. H_{so} is the spin-orbit (SO) coupling (ζ is the one electron SO parameter). H_{CF} is the crystal field Hamiltonian, which is represented for octahedral symmetry O_h in the Wybourne's notation by the following [18,19]:

$$H_{CF} = B_4^{oct}\left[C_0^{(4)} + \sqrt{\frac{5}{14}}\left(C_0^{(4)} + C_{-4}^{(4)}\right)\right] \quad (3)$$

B_4^{oct} is the octahedral CF parameter and C_q^k are the Racah tensor operators. The matrix elements of C_q^k operators are calculated numerically by the Racah tensor algebraic methods [20], whereas the Racah parameters B and C, the Trees parameter α, the crystal field parameter B_4^{oct} , and the one electron SO parameter ζ have to be determined from the optical spectra. The parameter Dq, characteristic of transition metals, shows the crystal field strength and is related to the $B_4{}^{oct}$ parameter by the relation: $10Dq = 21\ B_4{}^{oct}$.

The spin-orbit coupling term ζ is related to racah parameters B and C by the relation [21]:

$$\zeta = N^2\zeta_0 \text{ with } N^2 = \frac{1}{2}\left(\sqrt{\frac{B}{B_0}} + \sqrt{\frac{C}{C_0}}\right) \quad (4)$$

B_0= 918 cm^{-1} and C_0= 3850 cm^{-1} are the Racah parameters and ζ_0 = 273 cm^{-1} is the spin-orbit coupling coefficient of the free Cr^{3+} ion [22].

Since, the crystal-field is of the intermediate strength for $3d^N$ transition ions of the first series in crystals, [13,15,18] the basis functions $\{|d^N\ L\ S\ M_L M_S\rangle\}$ in the LS-coupling scheme have been adopted in our computer package. As a part of a larger project, we have set to develop a crystal field analysis computer program based on MAPLE software to calculate the energy levels and state vectors for any transition metal ion with the $3d^N$ configuration (N = 2, 3, 7, 8) located at sites with symmetry given by any of the 32 crystallographic point groups. This computer program has been tested and has given the same results as the one of Y. Yeung and C. Rudowicz [23].

4. Results And Discussion

The absorption spectrum of Cr^{3+} in BIGaZYTZr glass shows features due to the interaction between the $^2E_g(^2G)$ and $^2T_{1g}(^2G)$ sharp levels and the vibrationally $^4T_{2g}(^4F)$ quasicontinuum. The interactions between states of different spin multiplicities lead to interference dips. In this section, we first explain the origin of these dips in the model of adiabatic potential energy surface. Then, we analyze these features according to the Fano's antiresonance theory. Finally, we determine the electronic structure of Cr^{3+} in BIGaZYTZr by using the crystal field theory.

4.1. Adiabatic potential energy surface used to explain the interference dips

To explain the origin of the interference dips, we use the notion of adiabatic potential energy surfaces. In this model, we characterize the interference between the quartet $^4T_{2g}(^4F)$ and the doublet $^2E_g(^2G)$ excited states because it is an obvious dip in the absorption spectrum of Figure 1. We have not taking into account the interaction with the $^2T_{1g}(^2G)$ excited state because the values of the parameters that describe the interference dip for this state are more inaccurate due to the contribution from the $^4T_{1g}(^4F)$ excited state. The origin of the Fano's antiresonance is explained by the spin-orbit coupling between the two states $^4T_{2g}(^4F)$ and $^2E_g(^2G)$ [10-11]. In this qualitative study, each harmonic potential is defined along a single normal coordinate $\boldsymbol{Q}$ with its frequency $\boldsymbol{k}$ in wavenumber units. The position of the potential minimum and the vibrational frequency for the $^2E_g(^2G)$ state are identical to the ground state potential minimum $^4A_{2g}(^4F)$, set to $Q=0$. This doublet state is not displaced along the normal coordinate because the electronic transition corresponds to an intra-configurational d-d excitation [24-27]. The position of $^4T_{2g}(^4F)$ minimum is displaced along Q by an amount ΔQ and we consider its vibrational frequencies to be identical to those on the ground and doublet excited states. This quartet state surface is displaced to longer metal-ligand bond distances because the d-d excitation populates metal-ligand antibonding molecular orbitals [24-27]. The magnitude of the displacement ΔQ is determined from the width of the spin-allowed absorption band in the experimental spectrum. $E(^2E_g)$ and $E(^4T_{2g})$ are the energy of the potential minimum for $^2E_g(^2G)$ and $^4T_{2g}(^4F)$ states respectively. The potentials for the two excited states in the absence of spin-orbit coupling are given by :

$$V(^2E_g) = V_1 = \frac{1}{2}(k\,Q^2) + E(^2E_g) \quad (5)$$

$$V(^4T_{2g}) = V_2 = \frac{1}{2}(k\,(Q-\Delta Q\;)^2) + E(^4T_{2g}) \quad (6)$$

If we take into account the spin orbit coupling, the quartet excited state $^4T_{2g}(^4F)$ is split into four levels (2G, E_1 and E_2) and the doublet excited state just undergoes a displacement (G). The corresponding uncoupled potentials are called diabatic potentials. The interaction between the same symmetry levels (G) deriving from electronic states of different multiplicities leads to the observed spin-forbidden transition from $^4A_{2g}(^4F)$ ground state to $^2E_g(^2G)$ excited state. Effectively, the $^4T_{2g}(^4F)$ and $^2E_g(^2G)$ diabatic potentials are coupled by a constant V_{12} which its magnitude is on the order of the spin-orbit coupling constant ζ. These coupled potentials are called adiabatic potentials and are obtained by diagonalizing the following 2x2 potential matrix:

$$V(^2E_g,\ ^4T_{2g}) = \begin{pmatrix} V(^2E_g) & V_{12} \\ V_{12} & V(^4T_{2g}) \end{pmatrix} \quad (7)$$

The adiabatic potentials are given by the following expression [34]:

$$V_+ = \frac{1}{2}\left[(V_1+V_2) + \sqrt{(V_1-V_2)^2+4V_{12}}\right] \quad (8)$$

$$V_- = \frac{1}{2}\left[(V_1+V_2) - \sqrt{(V_1-V_2)^2+4V_{12}}\right] \quad (9)$$

where V_+ and V_- are the upper and lower adiabatic potentials. The adiabatic excited state surfaces are shown as solid lines and the dotted curves corresponding to the diabatic excited state potential energy as illustrated in Figure 2. The consideration of the spin orbit coupling between $^2E_g(^2G)$ and $^4T_{2g}(^4F)$ leads to the adiabatic excited state potential energy curves V_+ and V_- which are responsible of the spin-allowed $^4A_{2g}(^4F) \rightarrow {}^4T_{2g}(^4F)$ and the spin-forbidden $^4A_{2g}(^4F) \rightarrow {}^2E_g(^2G)$ transitions and permit us to explain the interference dip.

4.2. Fano's antiresonance study of $^4T_{2g}(^4F)$, $^2E_g(^2G)$ and $^2T_{1g}(^2G)$ states

The study of the interference dips can be made according to the Fano's antiresonance theory presented by Sturge *et al.* and Lempicki *et al.* [12,28].

The Fano's profile function R(ω) is obtained from the ration of the experimental absorption spectrum to the background spectrum, the latter calculated by fitting the wings of the spectrum by a single Gaussian function. Figure 1 shows the results of the Gaussian fit. The R(ω) curve and its fit from Eq. 1 is represented in Figure 3. The fitted parameters ρ_i^2, q_i, γ_i and ω_{oi} (i=1 for $^2E_g(^2G)$ state and i=2 for $^2T_{1g}(^2G)$ state) listed in Table 1. It can be observed that the Fano's antiresonances parameters obtained in this study are compatible with the result obtained by Illarramendi *et al.* for homologous fluoride glasses [29].

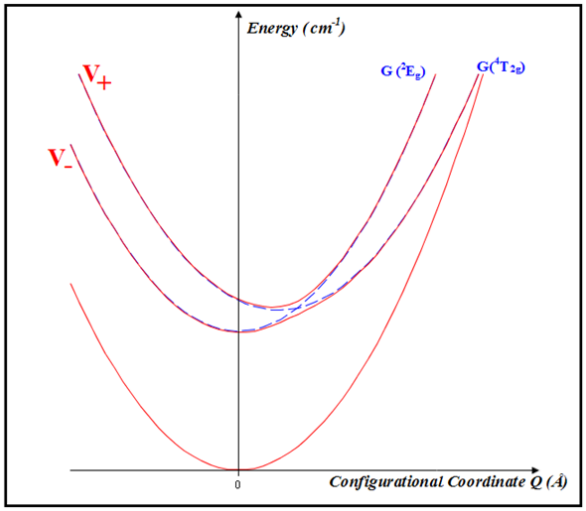

Figure 2. Potential energy curves for the $^4T_{2g}(^4F)$ and $^2E_g(^2G)$ excited states. The diabatic and adiabatic potentials for these electronic states are shown by dashed and solid lines respectively.

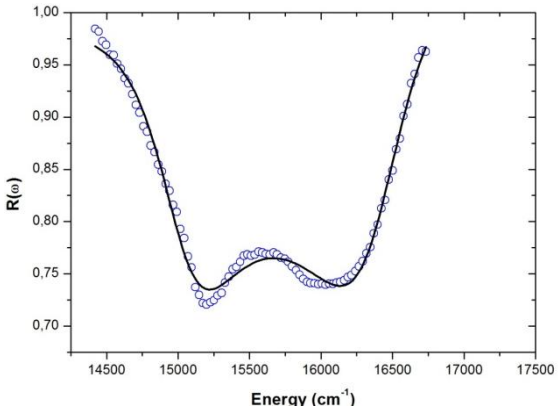

Figure 3. Experimental Fano's antiresonances profile (plotted line) and fits to Eq.1 (solid line) for Cr3+ doped BIGaZYTZr fluoride glass.

Table 1. Parameters of $^2E_g(^2G)$ and $^2T_{1g}(^2G)$ antiresonances for Cr^{3+}: BIGaZYTZr and comparison with homologous glasses.

	Parameter	Cr^{3+}: BIGaZYTZr	Cr^{3+}: BIGaZYT [31]	Cr^{3+}: BIZYT [31]
^2E_g	ρ_1^2	0.17	0.28	0.23
	q_1	-0.39	-0.219	-0.148
	$\gamma_1(cm^{-1})$	376	336	292
	$\omega_{1r}(cm^{-1})$	15 036	15 245	15 227
$^2T_{1g}$	ρ_2^2	0.20	-	-
	q_2	0.52	-	-
	$\gamma_2(cm^{-1})$	450	-	-
	$\omega_{2r}(cm^{-1})$	16 406	-	-

Table 2. Crystal field, Racah, trees and spin-orbit coupling parameters values for Cr3+doped BiGaZYTZr fluoride glass.

Material	Dq (cm^{-1})	B (cm^{-1})	C (cm^{-1})	B_4^{oct} (cm^{-1})	α	ζ (cm^{-1})
Cr^{3+}: BIGaZYTZr[a]	1540	787	3 045	32 340	70	248

The value obtained for ρ^2 parameter can be related to the larger disorder in glasses [28] which produces a more complete mixing of the spin-orbit components of the $^4T_{2g}(^4F)$ with components of ^2E_g (^2G) and $^2T_{1g}$ (^2G). The q parameter, ranging from -∞ to +∞, characterizes the line shape. The small value obtained for q indicates that the antiresonance is produced by a sharp forbidden transition overlapping with a broad allowed band. The value of γ indicates an inhomogenous broadening of the transition due to the presence of several environments in the glass. The last fitted parameter, ω_r, quantifies the position of the antiresonance in absorption and permits an estimation of the shift of the sharp levels due to coupling with the quasi-continuum. If we compare the values of ρ^2, it can be seen that the BIGaZYTZr fluoride glass has the smallest value and consequently should be the most ordered glass. The values of the antiresonance linewidths γ are influenced by the inhomogeneous broadening due to the presence of several environments in the glasses. The last fitted parameters, ω_{r1} and ω_{r2}, quantify the position of the antiresonances in absorption.

From the energy position of $^4T_{2g}(^4F)$, $^2E(^2G)$, $^2T_{1g}(^2G)$ and $^4T_{1g}(^4F)$ levels obtained by the Fano's antiresonance study we can performed the crystal field analysis on Cr^{3+} doped in BiGaZYTZr.

4.3. Crystal field study of the absorption spectrum of Cr^{3+}: BiGaZYTZr

The theoretical energies chromium Cr^{3+}: BIGaZYTZr are obtained by diagonalizing the full 120x120 matrix associated to the Hamiltonian of Eq. 1 in the free ion eigenstates $|LSM_LM_S\rangle$ within the quartet terms (^4F ground state and ^4P excited state) and doublet excited terms (^2H, ^2G, ^2F, ^2_aD, ^2_bD and ^2P). These energies are function of the B, C, α, B_4^{oct} and ζ parameters. From the absorption spectrum of Figure 1, we determine the 10Dq crystal field strength, it represents the difference between the excited state $^4T_{2g}(^4F)$ and the ground state $^4A_{2g}(^4F)$. The crystal field

parameter B_4^{oct} is then deduced from the value of 10Dq [13,30]. The Racah parameters B is obtained from the observed quartet state $^4T_{1g}(^4F)$.

The spin-orbit coupling term ζ is calculated from the Racah parameters B and C by Eq. 5. The Racah parameter C, the Trees correction α and parameters are adjusted using the Newton Raphson method to minimize the difference between the calculated and the observed $^2E_g(^2G)$ energy levels. The spin orbit parameter ζ is introduced in our computer package in order to obtain the splitting of the Stark levels of the O_h site symmetry. The set of calculated parameters B, C, B_4^{oct}, Dq, α and ζ listed in Table 2 permit as to deduce the calculated energy levels reported in Table3. The calculated and the experimental energies are in good agreements.

The electrostatic crystal field theory deals only with the d orbitals. The molecular orbitals are in reality influenced by the interaction between the ligand's s and p orbitals and the d orbitals of the central ion. The admixture of these orbitals leads to the s, σ and π bondings between the Cr^{3+} impurity ion and F ligands. Thus, the 10Dq parameter obtained from absorption spectra of Figure 1 contains the two contributions : the crystal field measure and also comprises the admixture of the antibonding e_g and t_{2g} orbitals with s and p ligand orbitals. The 10Dq parameter strongly depends upon the metal-ligand distance. The Racah parameters B and C are reduced compared to the free ion due to covalency effects.

The Tanabe-Sugano diagrams for Cr^{3+} ion in octahedral symmetry site of Figure 4 is drawn with the Racah parameters B and C of Table 1 (C/B=3.88). It indicates the general behavior of Cr^{3+} ion energy levels as a function of the local field strength measured in terms of Dq/B. The vertical line represents the appropriate value for Dq/B found for Cr^{3+} in BiGaZYT. From this diagram, we remark also that the $^4T_{2g}(^4F)$ quartet state and the ($^2E_g(^2G)$,$^2T_{1g}(^2G)$) doublet states are near for the calculated parameters Dq, B and C. This shows a strong coupling between the electronic states of different multiplicities. All these excited states are subdivided into E_1, E_2 and G states by spin-orbit coupling (Figure 5).

The interaction between the same symmetry levels (E_1, E_2 or G) deriving from electronic states of different multiplicities leads to the observed spin-forbidden transitions from the $^4A_{2g}(^4F)$ ground state to the $^2E_g(^2G)$ and the $^2T_{1g}(^2G)$ excited states (O_h symmetry) with lower intensity compared to a spin-allowed transition (Figure 5).

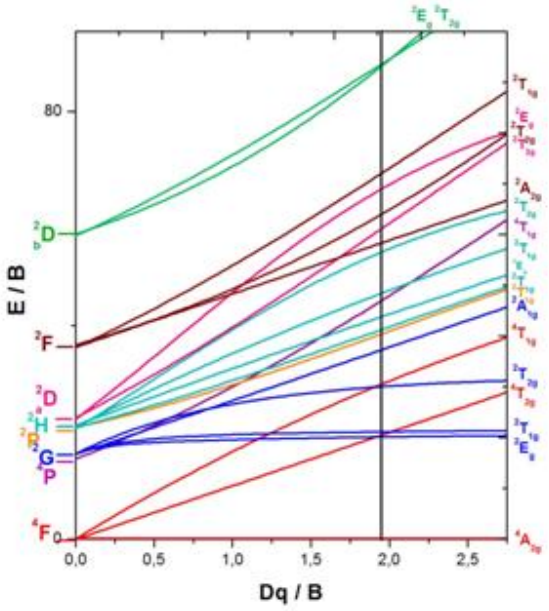

Figure 4. Tanabe-Sugano diagram for octahedrally coordinated Cr3+ ion with C/B=3.88. The vertical line represents the case of Cr3+ in BIGaZYTZr fluoride glass.

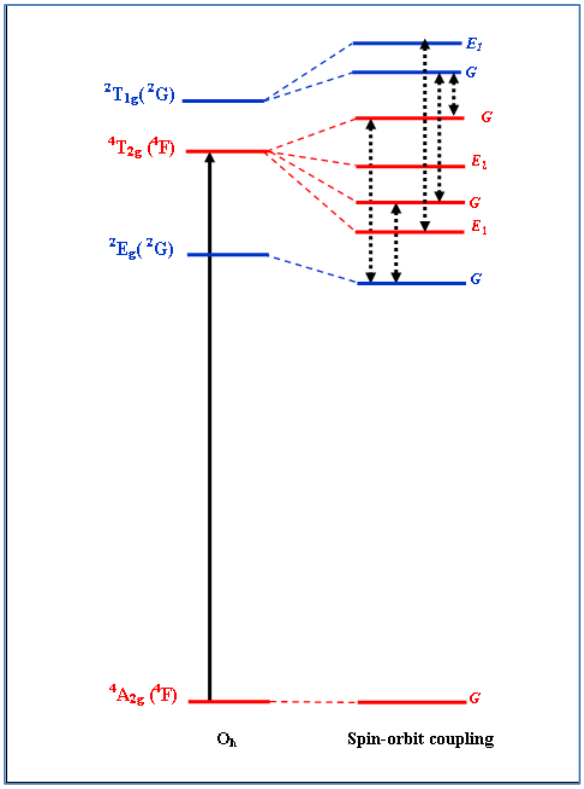

Figure 5. Electronic states of $^4T_{2g}(^4F)$, $^2E_g(^2G)$ and $^2T_{1g}(^2G)$ of Cr^{3+} in BIGaZYTZr fluoride glass. Solid arrows denote spin-allowed transition. Dotted arrows connect pairs of interacting levels under spin-orbit coupling.

Table 3. Experimental and calculated energies (cm^{-1}) of Cr^{3+} occupying a O_h symmetry in BiGaZYTZr fluoride glass (the " - " signifies that the states are not visible).

	Cr^{3+}: BiGaZYTZr			
O_h	E_{obs}	E_{cal}* [this work]	E^a_{cal}* [this work]	*mul**
$^4A_{2g}(^4F)$	0	0	0	4
$^2E_g(^2G)$	15 036	15 268	15 036	4
$^4T_{2g}(^4F)$	15 391	15 400	15 303	2
			15 365	4
			15 422	2
			15 653	4
$^2T_{1g}(^2G)$	16 406	16 029	16 030	4
			16 122	2
$^2T_{2g}(^2G)$	-	22 193	22 048	2
			22 050	4
$^4T_{1g}(^4F)$	22 423	22 422	22 454	4
			22 514	2
			22 530	4
			22 637	2
$^2A_{1g}(^2G)$	-	28 243	28 262	2
$^2T_{1g}(^2P)$	-	30 887	30 853	2
			30 908	4
$^2T_{1g}(^2H)$	-	31 239	31 112	2
			31 292	4
$^2E_g(^2H)$	-	32 777	32 776	4
$^4T_{1g}(^4P)$	-	34 883	34 882	4
			34 887	2
			34 908	4
			34 913	2
$^2T_{1g}(^2H)$	-	36 151	36 130	2
			36 240	4
$^2T_{2g}(^2H)$	-	41 529	41 527	2
			41 548	4
$^2A_{2g}(^2F)$	-	43 423	43 435	2
$^2T_{2g}(^2_aD)$	-	46 661	46 610	2
			46 718	4
$^2T_{2g}(^2F)$	-	47 945	47 845	2
			48 024	4
$^2E_g(^2_aD)$	-	51 132	51 147	4
$^2T_{1g}(^2F)$	-	53 659	53 596	2
			53 711	4
$^2E_g(^2_bD)$	-	69 234	69 239	4
$^2T_{2g}(^2_bD)$	-	69 280	69 262	4
			69 416	2

* *mul: multiplicity*

**E_{cal}: means the energies without spin orbit coupling.*

**E^a_{cal}: means the energies taking into account the spin-orbit coupling.*

By comparing the crystal field strength Dq of Cr^{3+}: BiGaZYTZr with those of homologous fluoride glasses of literature, we notice the decrease of the 10Dq parameter in the sense Dq(BIZYT) = 1550cm^{-1} [31] > Dq(BIGaZYT) =1548 cm^{-1} [31] > Dq(BIGaZYTZr) = 1540 cm^{-1}. The intensity of the crystal field Dq depends on the distortion of the polyhedron formed glass structural network. As the distortion is important then the distance between Cr^{3+}-F^- becomes large. Consequently, the crystal-field strength decreases. It is obvious that the value for Dq in glasses is determined primarily by the network structure glasses. In another way, the 10Dq parameter decreases as the number of fluoride ions increases. This suggests that this decrease results in larger Cr^{3+}-F^- distances.

For transition metal, the spin orbit constant λ is related to the effective g factor obtained from Electron Paramagnetic Resonance (EPR) by the expression [32] :

$$g_{eff} = g_e - \frac{8\lambda}{\Delta} \qquad (10)$$

Where : g_e= 2.0023 is the free electron factor, Δ is the gap between the excited and the ground levels (Δ = $E(^4T_2) - E(^4A_2)$ = 10Dq).

The S-O coupling constant λ is connected to the one-electron S-O coupling constant ξ by the following relation [33]

$$\lambda = \pm\frac{\xi}{2S} \qquad (11)$$

The sign + is valid for a layer less than half full and the sign - to a more than half-complete layer. For $3d^3$ electronic configuration (S=3/2), so we have ξ = 3λ.

From the theoretical values obtained by crystal Field analysis (Δ = 15400 $cm^{-1}$and λ = ξ /3=83cm^{-1}), we find g_{eff} = 1.95918

5.Conclusion

The features observed on the $^4T_{2g}(^4F)$ absorption band of Cr^{3+} in BIGaZYTZr glass are due to the interaction between the $^2E_g(^2G)$ and $^2T_{1g}(^2G)$ sharp levels and the vibrationally $^4T_{2g}(^4F)$ quasicontinuum. The model of the adiabatic potential energy surfaces explain the origin of interaction between different spin multiplicities states via spin orbit coupling. These features leading to the interference dips have been analyzed by the Fano's antiresonance model exposed by Sturge et al and Lempicki et al. The fitted parameters involved in this model give information about the fraction of the quasi-continuum which takes part in the interference

process and the line shape profile of the antiresonance. From these parameters and by comparison with other fluoride glasses: BIZYT and BIGaZYT, we deduce that the most order glass is the BIGaZYTZr fluoride glass. The electronic structure of Cr^{3+} occupying O_h site symmetry in the BIGaZYTZr glasses has been analyzed using the crystal field theory. The estimated parameters B, C, Dq, α and ζ lead to a good agreement between the calculated and observed levels.

Acknowledgments

The authors are indebted to Prof. Brigitte Boulard from **«Institut des Molécules et Matériaux de Mans »** for her scientific support and her constructive recommendations.

References

[1] M. M. Broer and L. G. Cohen, J. Lightwave Technol. 4 (1986) 1509-1513.
[2] L. Reekie, R. J. Mears, S. B. Poole, and D. N. Payne, J. Lightwave Technol. 4 (1986) 956-960.
[3] R. S. Quimby, M. G. Drexhage, and M. J. Suscavage, Electron. Lett. 23 (1987) 32-34.
[4] D. C. Yeh, W. A. Sibley, M. Suscavage, and M. G. Drexhage, J. Appl. Phys. 62 (1987) 266-275.
[5] M. G. Drexhage, in Treatise on Materials Science and Technology, edited by M. Tomozawa and R. H. Dorernus (Academic,New York, 1985), pp. 151- 243.
[6] P. T. Kenyon, L. J. Andrews, B. C. McCollum, and A. Lempicki, IEEE J. Quant. Electron. 18, (1982) 1189-1197.
[7] R. Reisfeld, Mater. Sci. Eng. 71 (1985) 375-382.
[8] M. J. Elejalde, R. Balda, J. Fernandez, and E. Macho, Phys. Rev. B 46 (1992) 5169-5182.
[9] C. BenHamideche, A. Boutarfaia and M. Poulain, J. of non-oxide glasses 1 (2009) 261-265.
[10] U. Fano Phys. Rev. 124 (1961) 1866-1878.
[11] U. Fano and J. W. Cooper 1965 Phys. Rev. 137 A1361.
[12] M. D. Sturge, H. J. Guggenheim, M. H. Pryce, Phys. Rev. B 2 (1970) 2459-2471.
[13] S. Sugano, Y. Tanabe, H. Kamimura, *Multiplets of transition-metal ions in crystals* (Academic Press, New York, 1970).
[14] J. S. Griffith, *The Theory of transition-metal ions* (Cambridge University Press, Cambridge, 1961).
[15] R. C. Powell, *Physics of Solid-State Laser Materials* (1thEd. Springer-Verlag, New York, 1998) pp.215-233.
[16] Z. Y. Yang, C. Rudowicz, and Y. Y. Yeung, Physica B 348 (2004) 151-159.
[17] C. Rudowicz, Z. Y. Yang, Y. Y. Yeung, and J. Qin, J. Phys. Chem. Solids 64 (2003) 1419-1428.
[18] D. J. Newman and B. Ng, *Crystal field Handbook* (1thEd. Cambridge University Press, 2000) pp.28-36.
[19] B. G. Wybourne, *Spectroscopic Properties of Rare Earth*(1thEd. Wiley, New York, 1965)pp.48-234.
[20] J. P. Elliott, B.R. Judd, W.A. Runciman, Proc. R. Soc. London, Ser. A 240 (1957) 509-523.
[21] M. G. Zhao, J. A. Xu, G. R. Bai and H. S. Xie, Phys. Rev. B 27 (1983) 1516-1522.
[22] Y. Tanabe and S. Sugano, J. Phys. Soc. Japan. 9 (1954) 766-779.
[23] Y. Y. Yeung, C. Rudowicz, Comput. Chem. 16 (1992) 207-216.
[24] J.I. Zink, J.Am.Chem.Soc. 94 (1972) 8039-8045.
[25] J.I. Zink, J.Am.Chem.Soc. 96 (1974) 4464-4470.
[26] L.G. VanQuickenborne and A. Ceulemans, Coord. Chem. Rev. 48 (1983) 157-202.
[27] J.I. Zink and K.K. Shin, « *Molecular distortions in Excited Electronic States determined from Electronic and Resonance Raman Spectroscopy* », in Advances in Photochemistry (Wiley, New York, 1991), pp119-214.
[28] A. Lempicki, L. Andrews, S. J. Nettel, B. C. McCollum and E. I. Solomon, Phys. Rev. Lett. 44 (1980) 1234-1237.
[29] M. A. Illarramendi, R. Balda, and J. Fernandez, Phys. Rev. B 47 (1993) 8411- 8417.
[30] Y. Tanabe and S. Sugano, J. Phys. Soc. Japan 9 (1954) 766-779.
[31] J. Fernández, M. A. Illarramendi and R. Balda, J. Non-Cryst. Solids 131-133 (1991) 1230-1234.
[32] Fuxi, G. Optical and Spectroscopic Properties of Glass;Springer: Berlin, 1992.
[33] Condon, E. U. and Shortley, G. H. The Theory of Atomic Spectra, University press, Cambridge and New York, 1935(reprinted 1951).